Title

Macular Vessel Density in Glaucomatous Eyes With Focal Lamina Cribrosa Defects

Journal

Journal of Glaucoma, 27(4)

ISSN

1057-0829

Authors

Ghahari, Elham
Bowd, Christopher
Zangwill, Linda M
et al.

Publication Date

2018-04-01

DOI

10.1097/ijg.0000000000000922

Peer reviewed

HHS Public Access

Author manuscript

J Glaucoma. Author manuscript; available in PMC 2019 April 01.

Published in final edited form as:

J Glaucoma. 2018 April ; 27(4): 342–349. doi:10.1097/IJG.0000000000000922.

Macular Vessel Density in Glaucomatous Eyes with Focal Lamina Cribrosa Defects

Elham Ghahari, MD[1], **Christopher Bowd, PHD**[1], **Linda M. Zangwill, PHD**[1], **Min Hee Suh, MD**[1,2], **Takuhei Shoji, MD, PHD**[1,3], **Kyle A. Hasenstab, PHD**[1], **Luke J. Saunders, PHD**[1], **Sasan Moghimi, MD**[1], **Huiyuan Hou, MD, PHD**[1], **Patricia Isabel C. Manalastas, MD**[1], **Rafaella C. Penteado, MD**[1], and **Robert N. Weinreb, MD**[1,*]

[1]Hamilton Glaucoma Center, Shiley Eye Institute, Department of Ophthalmology, University of California, San Diego, CA, United States

[2]Department of Ophthalmology, Haeundae Paik Hospital, Inje University, Busan, South Korea

[3]Department of Ophthalmology, Saitama Medical University. Iruma, Saitama, Japan

Abstract

PURPOSE—To compare optical coherence tomography angiography (OCTA) measured macular vessel density and spectral domain optical coherence tomography (SDOCT) measured macular ganglion cell complex (GCC) thickness in primary open-angle glaucoma (POAG) eyes with and without focal lamina cribrosa (LC) defects.

METHODS—In this cross-sectional, case-control study of patients with POAG, 46 eyes of 46 patients with LC defects and 54 eyes of 54 patients without observable LC defects were included. OCTA and SDOCT imaging were performed on the same day by the same operator. Perimetry and swept-source OCT testing used to identify LC defects were conducted within 6-months of OCTA and SDOCT testing. Global and local parafoveal vessel density (pfVD) and macular ganglion cell complex (mGCC) thickness were compared between study groups.

RESULTS—Glaucoma severity was similar between groups (SAP MD = −5.63 dB and -4.64 dB for eyes with and without LC defects, respectively; P = 0.40). Global and local measured pfVD was similar between groups (all P ≥ 0.11). GCC focal loss volume (GCC-FLV) was higher in eyes with LC defects than eyes without LC defects (7.2% and 4.97%, respectively; P = 0.03). In addition, GCC-FVL was topographically related to defect location in LC defect eyes.

*Corresponding author: Robert N. Weinreb, Hamilton Glaucoma Center, Department of Ophthalmology, University of California San Diego, La Jolla, California, rweinreb@ucsd.edu.

Commercial Disclosures:

1. L.M.Z: F: National Eye Institute, Carl Zeiss Meditec Inc., Heidelberg Engineering GmbH, Optovue Inc., Topcon Medical Systems Inc. C: Merck; R: Optovue, Topcon Medical Systems.
2. T.S: R: Alcon, Pfizer, Kowa, Otsuka, Santen, Senju
3. R.N.W.: C: Aerie Pharmaceutical, Alcon, Allergan, Bausch & Lomb, Eyenovia, Sensimed, Unity; F: Heidelberg Engineering, Carl Zeiss Meditec, Genentech, Optovue, Quark, Topcon.
4. C.B; M.H.S; K.H; L.J.S; S.M; H.H; P.I.C.M; R.C.P: None

CONCLUSIONS—Although OCTA macular vessel density was not significantly different between eyes with and without LC defects, focal GCC loss in eyes with LC defects was different. This highlights the importance of not relying solely on vessel density measurements for determining macular changes for diagnosing and detecting glaucomatous progression.

Keywords

Optical coherence tomography angiography; lamina cribrosa defect; open angle glaucoma; macula

INTRODUCTION

The pathogenesis of primary open angle glaucoma (POAG) is not fully understood but there is consistent evidence that both mechanical and vascular factors are involved.[1] Intraocular pressure (IOP), the most important risk factor for the development of POAG can cause mechanical stress on the posterior structures of the eye, notably the lamina cribrosa (LC) and adjacent tissues.[2] The sclera is perforated at the lamina, the weakest point in the eye wall, where retinal blood vessels and retinal ganglion cell axons exit the eye. IOP–induced stress may result in compression, deformation, and remodeling of the LC with consequent mechanical axonal damage [3] and disruption of retrograde delivery of essential trophic factors to retinal ganglion cells (RGC).[2]

Vascular factors also have a role in the pathogenesis of glaucoma. Glaucomatous optic neuropathy can occur in individuals with IOP within the normal range. In such patients, other risk factors such as abnormally low cerebrospinal fluid pressure in the optic nerve subarachnoid space resulting in a large pressure gradient across the lamina[4] or vascular dysfunction and decreased ocular perfusion pressure[5,6] may be causative factors and are under further investigation. With the recent introduction of optical coherence tomography angiography (OCTA) which has good reproducibility,[7] it is now possible to qualitatively and quantitatively assess retinal microvaculature at different retinal layers. [8–16]

In healthy eyes, the LC has a smooth, curvilinear anterior surface that is flat or that slopes slightly upward as it approaches the laminar insertion. In contrast, some glaucomatous eyes have thinning and posterior displacement of the LC[17,18] or localized irregularities of the anterior LC.[19,20] These focal LC defects likely represent localized loss of laminar tissue and correlate spatially with glaucomatous optic nerve head (ONH) structural changes [neuroretinal rim loss, optic nerve head pit and retinal nerve fiber layer (RNFL) defects], [21,22,23] glaucomatous visual field loss[19, 22] and ONH vascular changes such as ONH hemorrhage. [23,24,25]

Results indicate that compression, extension, or shearing of axons within the LC leads to axonal damage in the optic nerve head [2,3] and loss of RGCs. [26,27] For years, glaucoma was considered to affect primarily the optic nerve head and corresponding peripheral visual field. However recent evidence has shown that early glaucoma also is associated with damage to RGCs in the macula that can be demonstrated during testing of the central visual field. [28,29]

Recently, a topographic association between focal LC defects and deep layer peripapillary microvasculature dropout has been observed.[30] We have reported that OCTA deep layer

ONH peripapillary vessel density is significantly lower in POAG eyes with focal LC defects compared to eyes without focal LC defects with a similar severity of glaucoma (defined by MD) and similar RNFL thickness.[31] However, the extent of macular defects in glaucomatous eyes with and without focal LC defects has not yet been demonstrated. The purpose of the current study was to compare OCTA macular vessel density and macular thickness between POAG eyes with and without focal LC defects.

METHODS

This was a cross-sectional study of POAG patients enrolled in the Diagnostic Innovations in Glaucoma Study (DIGS). The DIGS is an ongoing prospective, longitudinal study at the Hamilton Glaucoma Center, University of California, San Diego, designed to evaluate optic nerve structure and visual function in glaucoma. Details of the DIGS protocol have been described previously.[32] All methods adhered to the tenets of the Declaration of Helsinki and the Health Insurance Portability and Accountability Act and were approved by the Institutional Review Board/Human Research Protections Program at the University of California, San Diego. Informed consent was obtained from all participants.

Patients with established POAG (as defined below) underwent ophthalmological examination, including assessment of best-corrected visual acuity (BCVA), slit- lamp biomicroscopy, IOP measurement with Goldmann applanation tonometry, gonioscopy, central corneal thickness (CCT) measured with ultrasound pachymetry (DGH Technology Inc., Exton, PA), dilated fundus examination, simultaneous stereophotography of the optic disc, and standard automated perimetry (Humphrey Field Analyzer; 24-2 using the Swedish Interactive Thresholding Algorithm; Carl Zeiss Meditec, Dublin, CA).

Avanti AngioVue (Optovue Inc. Fremont, CA) OCTA imaging and spectral-domain OCT (SDOCT) imaging were performed on the same day by the same operator. Perimetry and swept-source OCT (SSOCT, images used to identify LC defects) testing was conducted within 6-months of OCTA and SDOCT testing.

Inclusion criteria were as follows: patients diagnosed with POAG, aged > 18 years, BVCA ≥ 20/40, with open angles on gonioscopy. Those with systemic hypertension and diabetes mellitus without diabetic or hypertensive retinopathy were included.

Patients with a history of ocular intervention other than uncomplicated cataract or glaucoma surgery, intraocular disease (e.g., diabetic retinopathy or non- glaucomatous optic neuropathy), systemic disease that could have had impact on the study results (e.g., stroke or pituitary tumor) were excluded. Unreliable visual field (VF) results, or poor quality OCTA, SDOCT or SSOCT scans were not included in the analyses.

Systolic and diastolic blood pressure and pulse rate were measured with an Omron Automatic blood pressure instrument (model BP791IT; Omron Healthcare, Inc., Lake Forest, IL) just prior to OCTA imaging in the same seated position. Mean arterial pressure was calculated as 1/3 systolic blood pressure + 2/3 diastolic blood pressure. Mean ocular perfusion pressure was defined as the difference between 2/3 of mean arterial pressure and IOP.

POAG was defined as glaucomatous appearance of the optic nerve head (focal thinning, notching, or localized or diffuse atrophy of the RNFL) with associated repeatable VF damage. Glaucomatous VF damage was defined as a Glaucoma Hemifield Test outside of normal limits or a pattern standard deviation outside 95% normal limits confirmed on two consecutive, reliable (fixation losses and false-negatives 33% and 15% false-positives) tests.

The AngioVue system (software version 2015.1.0.35) incorporated in the Avanti SD-OCT system was used to measure vessel density. This system uses a split-spectrum amplitude-decorrelation angiography (SSADA) method to capture the motion contrast of the red blood cells to provide a high-resolution 3-dimensional visualization of the vascular structures at various user-defined layers of the retina at the capillary level.[8–16] The OCTA image is directly derived from SDOCT B-scans. The SDOCT image consists of a series of B-scans with two rapid repeats at each B-scan location, and the average of the two repeated B-scans forms the conventional SDOCT intensity image. The amplitude decorrelation between these two B-scans forms the OCTA image.[8] Because the OCTA tissue thickness measurements and SDOCT vessel density measurements are obtained from the same B-scans, there is pixel-to-pixel co-localization between image and therefore post-processing alignment is unnecessary.

We used peripapillary vessel density from the images acquired with a 4.5 × 4.5 mm^2 field of view centered on the optic disc. The ONH OCTA scanning protocol consists of a merged Fast-X volume of 304 horizontal B-scans of 304 A-scans per B-scan and a Fast-Y volume of 304 horizontal B-scans of 304 A-scans per B-scan. Macular vessel density measurements were calculated from 3 × 3 mm^2 scans centered on the fovea. The macula OCTA scanning protocol consists of a merged Fast-X volume of 304 horizontal B-scans of 304 A-scans per B-scan and a Fast-Y volume of 304 horizontal B-scans of 304 A-scans per B-scan. For both regions, segmentation was performed using the OCT intensity B-scans. Peripapillary vessel density measurements were calculated in a slab from the ILM to the posterior border of RNFL. Macular superficial vessel density measurements were calculated in a slab from the ILM to the posterior border of the IPL.

Circumpapillary vessel density (cpVD) was calculated under a 750 μm wide elliptical annulus extending from the optic disc boundary. Global (360°) vessel density measurement and eight sectoral (45° per sector) vessel densities measurements were assessed for analysis. Parafoveal vessel density (pfVD) was measured in an elliptical annulus with an inner diameter of 1 mm and outer diameter of 2.5 mm centered on the fovea (Figure 1). Global (360°) vessel density and four sectoral (90° per sector) vessel densities were assessed for analysis

The Avanti SDOCT system was used for imaging macular thickness. Avanti SDOCT has an A-scan rate of 70 kHz and a light source with a center wave length of 840 nm. The macular ganglion cell scanning protocol was used to measure the macular ganglion cell complex (mGCC) thickness. Software provided mGCC analysis parameters investigated were global loss volume (GCC-GLV) and focal loss volume (GCC-FLV).[33] The mGCC scanning protocol consists of a 7 × 7 mm^2 raster scan composed of 1 horizontal B scan of 933 A-scans and 15 vertical B scans of 933 A-scans per B-scan. This protocol measures retinal

thickness from the internal limiting membrane (ILM) to the inner plexiform layer (IPL) posterior boundary. Macular GCC thickness measurements consist of the ganglion cell layer, IPL, and RNFL. Good-quality images were defined as scans with a signal strength index ≥ 37 without segmentation failure or artifacts (missing or blank areas).

Trained graders reviewed the quality of all OCTA scans using a standard protocol established by the UCSD Imaging Data Evaluation and Analysis Center. Poor-quality scans were excluded from the analysis if one of the following criteria were met: (1) signal strength index of < 48; (2) poor-clarity images; (3) local weak signal caused by artifacts such as floaters; (4) residual motion artifacts visible as irregular vessel patterns or disc boundary on the enface angiogram; and (5) RNFL segmentation failure.

As described previously,[31] focal LC defects were identified from SSOCT (DRI-OCT; Topcon, Tokyo, Japan) optic disc scans. A 3-dimensional raster scan consisting of 256 serial horizontal B-scans over a 12 mm × 9 mm cube centered on the posterior pole (wide- field protocol) was acquired, and serial *en face* images were obtained from the 3-dimensional data set. After excluding poor-quality images (poorly focused, clipped or quality score < 50) and eyes with poor LC visibility (< 70% visibility of the anterior laminar surface within the Bruch's membrane opening), two masked independent observers (M.H.S. and P.I.C.M.) reviewed images to identify focal LC defects and discrepancies in identification were resolved by consensus. Images were excluded from the study if consensus could not be reached.

A laminar disinsertion or hole, violating the normal U- or W-shaped contour of the anterior laminar surface present on at least two consecutive scans, >30 mm in depth, and ≥100 mm in diameter, was defined as a focal LC defect. [19,21,22,23,25] In order to differentiate hypo-reflectivity due to vascular shadowing or true LC defect, the *en face* images were compared with the stereoscopic optic disc photographs.

LC defect location was identified in terms of eight 45-degree sectors corresponding to the sectors on the SDOCT Avanti and AngioVue instruments (Figure 2). An 8-sector circle was placed around the ONH on the SSOCT enface image after registering its location with that of the AngioVue cpVD circular diagram by matching the location of the vessels. In subjects with LC defect over two neighboring sectors, the one sector with the larger defect was included in the analysis.

As described previously,[31] one eye was randomly selected if both eyes of each patient were free of focal LC defects or had focal LC defects. In order to increase sample size, the eye with the focal LC defect was included if a patient had one eye with and one eye without a focal LC defect. Subjects without a focal LC defect were matched to those with defects for VF mean deviation (MD) by frequency matching to minimize the influence of the glaucoma severity on LC defect, cpRNFL thickness, and vessel density. Specifically, patients with focal LC defects were matched to patients without LC defect in 3 severity bins based on VF MD: early POAG (MD > −6 dB), moderate POAG (MD from −6 dB to −12 dB) and advanced POAG (MD < −12 dB).

STATISTICAL ANALYSES

Clinical characteristics, OCTA vessel densities and SDOCT thicknesses were compared between glaucomatous eyes with and without focal LC defects. The normality assumption was assessed by inspecting histograms. An independent samples Student's t-test was used for group comparison for normally distributed variables, the Mann-Whitney test or Wilcoxon test was used for continuous non-normal variables, and the chi-square test was used for categorical variables. All statistical analyses were performed with JMP Pro version 12 (SAS Institute Inc., Cary, NC). The alpha level (type I error) was set at 0.05.

RESULTS

After frequency matching for severity of POAG by VF MD, 46 eyes of 46 patients with focal LC defects and 54 eyes of 54 patients without LC defects were included in the analysis. As reported previously, there was an excellent interobserver agreement in determining the presence of the LC defect in this study population (Kappa = 0.84; 95% confidence interval, 0.76–0.91; $P < 0.001$).[31] Demographics and ocular characteristics of the study groups are summarized in Table 1. The two study groups were comparable in terms of age, race, systemic and ocular characteristics, and glaucoma disease severity (as defined by average RNFL thickness in addition to VF MD).

Table 2 presents the OCTA measured macular vessel densities and SDOCT measured macular thickness in eyes with and without LC defects. Eyes with and without a focal LC defect had similar macular OCTA vessel densities (51.62% and 50.86 %, respectively; P= 0.363) and mGCC thickness (80.79 μm and vs 81.33 μm, respectively; P= 0.817). In contrast, there was a higher GCC-FLV in eyes with LC defect compared to eyes without one (7.21% vs 4.97%, respectively; P=0.032).

Of the 46 eyes with LC defects, 29 had defects in only the inferotemporal region, 7 had defects in only the superotemporal region and 10 eyes had defects in both the inferotemporal and superotemporal regions. In subgroup analyses of eyes with (39 eyes) and without LC defects in the inferotemporal region, the only significantly different parameter in terms of macular thickness and vessel density was GCC-FLV [7.34% ± 5.60% (5.49%, 9.18%) vs 5.15% ± 4.74% (3.93%, 6.36%), P=0.040]. Subgroup analyses of 17 eyes with a LC defect in the superotemporal sector with the eyes without a defect in that sector showed no statistically significant differences in terms of macular vessel density and thickness.

The association between peripapillary vessel density in the same sector as the defect was evaluated. In eyes with a LC defect in the IT sector, IT circumpapillary vessel density was correlated with inferior macular vessel density (R^2=0.293, P=0.0004) and inferior average macular thickness (R^2=0.165, P=0.011). Although eyes with a ST LC defect were correlated with the corresponding area of macula thickness (i.e. superior average macular thickness (R^2=0.573, P=0.0004)), the topographic relationship was not significant for macular vessel density (Table 3).

DISCUSSION

This study compared macular vessel density measurements in POAG eyes with and without focal LC defects using OCTA. Macular vessel density parameters (wiVD, pfVD) in POAG eyes with and without focal LC defect were not significantly different. Until now, there has been sparse information of the utility of OCTA vessel density in POAG with and without LC defect, especially with regards to macular vessel density. This study now offers some novel insights into the impact of LC defects on macular vessel density.

Previous work has shown that focal LC defects and impaired ocular hemodynamics may be etiologically related and inseparable in glaucomatous optic nerve injury. [34] Further our group recently showed that OCTA peripapillary vessel density was significantly lower in POAG eyes with focal LC defects compared to eyes without LC defects. In addition, reduction of peripapillary vessel density was spatially correlated with the location of the LC defect.[31] In the current study, macular vessel density parameters (wiVD, pfVD) were not significantly different in POAG eyes with and without focal LC defects.

For this study, the sample size was larger than in our earlier study.[31] Assuming a similar difference in measurements between groups and a similar variability within groups for circumpapillary OCTA vessel density measurements, we would have had 80% power to detect a significant change with 48 eyes per group. In a recent study, [35] the standard deviation of pfVD in glaucoma eyes was smaller than the standard deviation of cpVD; this suggests that our calculated power is conservative. The pfVD standard deviation in the previous study was actually almost identical to that of the current study[35] (both 4.2%). A difference of 2.8%[35] would be detectable with 90.8% power; a sample size of 39 eyes per group would have been sufficient for 80% power. A 3.8% difference with this variability estimate[31] would be detectable with 99.6% power. To detect a smaller difference between groups of 2.5%, 49 eyes per group would be needed with 80% power. In this study, the difference in pfVD between eyes with LC defect and without was substantially smaller than what would have been expected from previous studies (0.79%). Moreover, with such a magnitude of difference, it is not likely to be clinically meaningful even if there were a large enough sample for this difference to be statistically significant given the variability of the measurement.

In terms of macular vessel density in glaucomatous eyes, our result is different from reported in other studies, because we did not find any difference between study groups. Reduced macular vessel density has been reported in the perimetrically intact hemiretinae of glaucoma eyes with a single-hemifield defect.[35] A recent study by Liu et al.[36] compared OCTA retinal vasculature measurements between nonarteritic anterior ischemic optic neuropathy (NAION) and open angle glaucoma (OAG) with altitudinal hemifield visual field defects. The NAION group demonstrated a marked decrease in cpVD while the OAG group demonstrated a significant decrease in pfVD.

One possible explanation for the observed lack of association between the presence of LC defects and parafoveal vessel density defects is that the effect of the LC defect is more localized with ONH vessel density. Loss of structural support of the laminar beams due to

the focal LC defect may directly or indirectly influence the local retinal microvasculature. [23] Conversely, impaired vascular supply to the laminar beams may lead to the focal disruption of the laminar structures.

The microcirculation of the retina and choroid are end-arterial systems without anastomoses. [37] The central retinal artery (CRA) supplies the retinal circulation while the short posterior ciliary arteries (SPCAs) supply the choroidal circulation. In a recent study by Yu et al.,[38] a close inter-relationship of the blood supply to the ONH, retina, and choroid was demonstrated. With fluorescent probes perfused via either the CRA or the SPCAs, they demonstrated that appeared blood can flow between the retinal and the choroidal vasculature. This suggests that blood flow via either the CRA or SPCAs can supply the vasculature in the retina, choroid, and the ONH, indicating extensive potential collateral pathways. The existence of an interplay between the blood supply to the ONH, retina, and choroid can explain why the vascular damage in the glaucoma eyes with focal LC defects is more localized around the optic nerve and there was no widespread damage that involve the macular vessel density according to our study.

Macular thickness measurements also were compared in these two study groups. They were not statistically different between eyes with LC defect and those without for most measurements. Only GCC-FLV (%) was different between the two groups, but the relatively high p-value (p=0.032) combined with the lack of significant differences between other variables suggests that this could be an artefact of multiple comparisons. Moreover, a recent longitudinal study suggests that at least in some eyes, macular microvascular dropout is detectable before GCC thinning. [31]. However, given that a number of studies suggest that GCC-FLV is one of the most reliable predictors for glaucoma progression in SDOCT measurements, [39, 40] it is perhaps worth investigating this relationship further with a larger sample size. In the current study, we were able to identify and recruit only a limited number of eyes with localized lamina cribrosa defects. This is not surprising as a recent study identified only 20 eyes with localized LC defects from a sample of 182 glaucoma eyes (6.6%) using swept-source OCT. [41]

One possible explanation for such a phenomenon if it does exist is that the focal structural loss may be a more reliable indicator of early glaucoma damage than diffuse thinning, which is more likely to be a normal anatomical variant.[42] Furthermore, the macular GCC is mapped over a wider area (7×7 mm^2) than macular vessel density measurements (3×3 mm^2) which may allow for a more sensitive detection of focal loss. Finally, focal loss that involves the macula may be a common pattern of glaucoma damage and may be reflective of the increased vulnerability of the inferotemporal disc and inferior macula or superior visual field.[19,21,29]

Subgroup analysis in eyes with LC defects localized to ONH inferotemporal sectors showed that the inferotemporal peripapillary vessel density is associated with vascular (wiVD, pfVD, inferior hemifield and inferior vessel density) and thickness (mGCC, GCC-FLV, GCC-GLV) parameters. In eyes with LC defects localized to ONH superotemporal sectors, superotemporal peripapillary vessel density was associated with macular thickness

parameters but not macular vessel densities. One possible explanation for this topographic association, could be the concept of macular vulnerability zone in glaucoma. [28,29]

This study has several possible limitations. First, the identification of focal LC defects was based on subjective observation and it is sometimes challenging to visualize the deep ONH structures. However, this limitation was addressed at least in part by having two graders determine the presence of LC defects and the excellent interobserver agreement in determining the presence of the LC defect (kappa = 0.84). Secondly, two different devices were used for image acquisition, so some may argue that they cannot be accurately related in terms of LC defect location and vessel density. The current SDOCT (Avanti) in which OCTA (AngioVue) software is incorporated does not have an enhanced depth imaging technique to image LC, so it was necessary to use another instrument for LC imaging that allows detailed analysis of the laminar structure. Therefore, SSOCT was used for the lamina analysis. However, the OCTA image is directly derived from SDOCT B-scans. SSOCT and SDOCT images were aligned by matching the large vessels, so it is unlikely that there is a significant error in evaluating the topographic relationship between vessel density and focal LC defects. Finally, this study was cross-sectional and non-interventional and because of that, we could not detect any cause and effect relationship. Also, we were not able to evaluate the potentially confounding impact of anti-glaucoma drops, BP-lowering medications, and systemic conditions on the vascular measurements. Therefore, despite the absence of differences in BP, IOP, or MOPP measurements between our study populations, one cannot dismiss the effect of these factors on vascular measurements. Effects of ocular and systemic conditions and the use of medications on vascular measurements is a topic for further studies.

In conclusion, in POAG eyes with comparable severity of glaucomatous damage, macular vessel density was similar between eyes with and without focal LC defects. However, a significant difference was found in GCC-FLV between POAG eyes with and without LC defects. These results suggest that OCTA and structural measurements of the macula are complementary, and highlight the importance of not relying solely on OCTA macular vessel density for determining the possible influence of lamina defects on the macula for diagnosing and detecting progression of glaucoma.

Acknowledgments

FUNDING/SUPPORT: Supported in part by National Institutes of Health/National Eye Institute grants EY11008, P30 EY022589, EY026590, EY027510, EY026574 (L.M.Z.), EY022039, EY027945 (C.B.), EY023704, EY029058 (R.N.W.), P30 EY022589 (K.A.H), and participant retention incentive grants in the form of glaucoma medication at no cost from Alcon Laboratories Inc, Allergan, Alcon, Pfizer Inc, and Santen Inc. Unrestricted grant from Research to Prevent Blindness, New York, New York.

References

1. Weinreb RN, Khaw PT. Primary open-angle glaucoma. Lancet. 2004; 363:1711–1720. [PubMed: 15158634]
2. Quigley HA, Addicks EM, Green WR, et al. Optic nerve damage in human glaucoma, II: the site of injury and susceptibility to damage. Arch Ophthalmol. 1981; 99:635–649. [PubMed: 6164357]
3. Fechtner RD, Weinreb RN. Mechanisms of optic nerve damage in primary open angle glaucoma. Surv Ophthalmol. 1994; 39:23–42. [PubMed: 7974188]

4. Wang N, Xie X, Yang D, et al. Orbital cerebrospinal fluid space in glaucoma: the Beijing Intracranial and Intraocular Pressure (iCOP) study. Ophthalmology. 2012; 119:2065–2073. [PubMed: 22749084]
5. Leske MC, Wu SY, Hennis A, et al. Risk factors for incident open-angle glaucoma: the Barbados Eye Studies. Ophthalmology. 2008; 115:85–93. [PubMed: 17629563]
6. Leske MC, Heijl A, Hyman L, et al. Predictors of long-term progression in the Early Manifest Glaucoma Trial. Ophthalmology. 2007; 114:1965–1972. [PubMed: 17628686]
7. Manalastas PIC, Zangwill LM, Saunders LJ, et al. Reproducibility of Optical Coherence Tomography Angiography Macular and Optic Nerve Head Vascular Density in Glaucoma and Healthy Eyes. J Glaucoma. 2017; 26:851–859. [PubMed: 28858159]
8. Jia Y, Wei E, Wang X, et al. Optical coherence tomography angiography of optic disc perfusion in glaucoma. Ophthalmology. 2014; 121:1322–1332. [PubMed: 24629312]
9. Yu J, Jiang C, Wang X, et al. Macular perfusion in healthy Chinese: an optical coherence tomography angiogram study. Invest Ophthalmol Vis Sci. 2015; 56:3212–3217. [PubMed: 26024105]
10. Liu L, Jia Y, Takusagawa HL, et al. Optical coherence tomography angiography of the peripapillary retina in glaucoma. JAMA Ophthalmol. 2015; 133:1045–1052. [PubMed: 26203793]
11. Zhang M, Hwang TS, Dongye C, et al. Automated Quantification of Nonperfusion in Three Retinal Plexuses Using Projection-Resolved Optical Coherence Tomography Angiography in Diabetic Retinopathy. Invest Ophthalmol Vis Sci. 2016; 57:5101–5106. [PubMed: 27699408]
12. Matsunaga DR, Yi JJ, De Koo LO, et al. Optical Coherence Tomography Angiography of Diabetic Retinopathy in Human Subjects. Ophthalmic Surg Laser Imaging Retina. 2015; 46:796–805.
13. Sulzbacher F, Pollreisz A, Kaider A, et al. Identification and clinical role of choroidal neovascularization characteristics based on optical coherence tomography angiography. Acta Ophthalmol. 2017; 95:414–420. [PubMed: 28133946]
14. Shahlaee A, Samara WA, Hsu J, et al. In Vivo Assessment of Macular Vascular Density in Healthy Human Eyes Using Optical Coherence Tomography Angiography. Am J Ophthalmol. 2016; 165:39–46. [PubMed: 26921803]
15. Lee J, Moon BG, Cho AR, et al. Optical Coherence Tomography Angiography of DME and Its Association with Anti-VEGF Treatment Response. Ophthalmology. 123(11):2368–2375.
16. Spaide RF, Klancnik JM Jr, Cooney MJ. Retinal vascular layers imaged by fluorescein angiography and optical coherence tomography angiography. JAMA Ophthalmol. 2015; 133:45–50. [PubMed: 25317632]
17. Agoumi Y, Sharpe GP, Hutchison DM, et al. Laminar and prelaminar tissue displacement during intraocular pressure elevation in glaucoma patients and healthy controls. Ophthalmology. 2011; 118:52–99. [PubMed: 20656352]
18. Park HY, Jeon SH, Park CK. Enhanced depth imaging detects lamina cribrosa thickness differences in normal tension glaucoma and primary open-angle glaucoma. Ophthalmology. 2012; 119:10–20. [PubMed: 22015382]
19. Kiumehr S, Park SC, Syril D, et al. In vivo evaluation of focal lamina cribrosa defects in glaucoma. Arch Ophthalmol. 2012; 130:552–559. [PubMed: 22232364]
20. Shoji T, Kuroda H, Suzuki M, et al. Correlation between lamina cribrosa tilt angles, myopia and glaucoma using OCT with a wide band width femtosecond mode-locked laser. Plos One. 2014; 9(12):e116305. doi:10.137. [PubMed: 25551632]
21. Tatham AJ, Miki A, Weinreb RN, et al. Defects of the lamina cribrosa in eyes with localized retinal nerve fiber layer loss. Ophthalmology. 2014; 121:110–118. [PubMed: 24144452]
22. You JY, Park SC, Su D, et al. Focal lamina cribrosa defects associated with glaucomatous rim thinning and acquired pits. JAMA Ophthalmol. 2013; 131:314–320. [PubMed: 23370812]
23. Park SC, Hsu AT, Su D, et al. Factors associated with focal lamina cribrosa defects in glaucoma. Invest Ophthalmol Vis Sci. 2013; 54:8401–8407. [PubMed: 24255039]
24. Sharpe GP, Danthurebandara VM, Vianna JR, et al. Optic disc hemorrhages and laminar disinsertions in glaucoma. Ophthalmology. 2016; 123:1949–1956. [PubMed: 27432205]
25. Kim YK, Park KH. Lamina cribrosa defects in eyes with glaucomatous disc haemorrhage. Acta Ophthalmol. 2016; 94:468–473.

26. Sigal IA, Flanagan JG, Tertinegg I, et al. Modeling individual-specific human optic nerve head biomechanics, part I: IOP-induced deformations and influence of geometry. Biomech Model Mechanobiol. 2009; 8:85–98. [PubMed: 18309526]
27. Sigal IA, Flanagan JG, Tertinegg I, et al. Predicted extension, compression and shearing of optic nerve head tissues. Exp Eye Res. 2007; 85:312–322. [PubMed: 17624325]
28. Hood DC, Raza AS, deMoraes CG, et al. Glaucomatous damage of the macula. Prog Retin Eye Res. 2013; 32:1–21. [PubMed: 22995953]
29. Hood DC. Improving our understanding, and detection, of glaucomatous damage: An approach based upon optical coherence tomography (OCT). Prog Retin Eye Res. 2017; 57:46–75. [PubMed: 28012881]
30. Suh MH, Zangwill LM, Manalastas PI, et al. Deep Retinal Layer Microvasculature Dropout Detected by the Optical Coherence Tomography Angiography in Glaucoma. Ophthalmology. 2016; 123:2509–2518. [PubMed: 27769587]
31. Suh MH, Zangwill LM, Manalastas PI, et al. Optical coherence tomography angiography vessel density in glaucomatous eyes with focal lamina cribrosa defects. Ophthalmology. 2016; 123:2309–2317. [PubMed: 27592175]
32. Sample PA, Girkin CA, Zangwill LM, et al. The African Descent and Glaucoma Evaluation Study (ADAGES): design and baseline data. Arch Ophthalmol. 2009; 127:1136–1145. [PubMed: 19752422]
33. Tan O, Chopra V, Lu AT, et al. Detection of macular ganglion cell loss in glaucoma by Fourier-domain optical coherence tomography. Ophthalmology. 2009; 116:2305–2314. [PubMed: 19744726]
34. Downs, C., Roberts, MD., Burgoyne, CF. Mechanical strain and restructuring of the optic nerve head. In: Shaarawy, TM.Sherwood, MB.Hitchings, RA., Crowston, JG., editors. Glaucoma Medical Diagnosis and Therapy. Vol. 1. Philadelphia, PA: Saunders Elsevier; 2009.
35. Yarmohammadi A, Zangwill LM, Diniz-Filho A, et al. Peripapillary and Macular Vessel Density in Patients with Glaucoma and Single-Hemifield Visual Field Defect. Ophthalmology. 2017; 124:709–719. [PubMed: 28196732]
36. Liu CH, Wu WC, Sun MH, et al. Comparison of the Retinal Microvascular Density Between Open Angle Glaucoma and Nonarteritic Anterior Ischemic Optic Neuropathy. Invest Ophthalmol Vis Sci. 2017; 58:3350–3356. [PubMed: 28687846]
37. Hayreh SS. Segmental nature of the choroidal vasculature. Br J Ophthalmol. 1975; 59:631–648. [PubMed: 812547]
38. Yu PK, McAllister IL, Morgan WH, et al. Inter relationship of arterial supply to human retina, choroid, and optic nerve head using micro perfusion and labeling. Invest Ophthalmol Vis Sci. 2017; 58:3565–3574. [PubMed: 28715592]
39. Zhang X, Loewen N, Tan O, et al. Advanced Imaging for Glaucoma Study Group. Predicting Development of Glaucomatous Visual Field Conversion Using Baseline Fourier-Domain Optical Coherence Tomography. Am J Ophthalmol. 2016; 163:29–37. [PubMed: 26627918]
40. Loewen NA, Zhang X, Tan O, et al. Combining measurements from three anatomical areas for glaucoma diagnosis using Fourier-domain optical coherence tomography. Br J Ophthalmol. 2015; 99:1224–1229. [PubMed: 25795917]
41. Takayama K, Hangai M, Kimura Y, et al. Three-dimensional imaging of lamina cribrosa defects in glaucoma using swept-source optical coherence tomography. Invest Ophthalmol Vis Sci. 2013; 54:4798–4807. [PubMed: 23778878]
42. Shoji T, Sato H, Ishida M, et al. Assessment of glaucomatous changes in subjects with high myopia using spectral domain optical coherence tomography. Invest Ophthalmol Vis Sci. 2011; 52:1098–1102. [PubMed: 21051712]

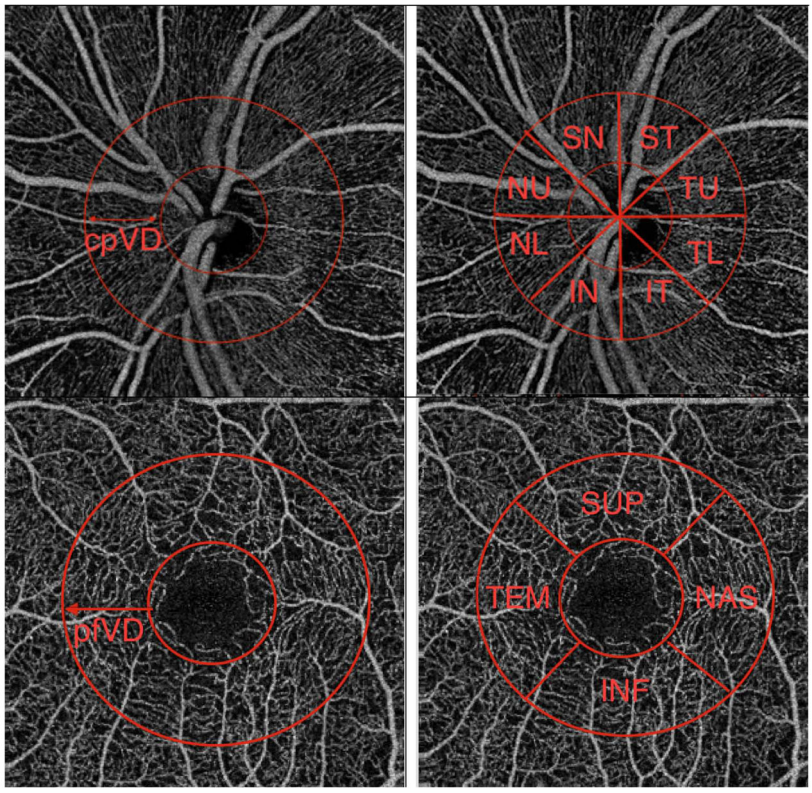

Figure 1.

Optical coherence tomography angiography (OCT-A) retinal nerve fiber layer vessel density map of optic nerve head (top) and macula (bottom) and corresponding segmentation that have been used in this study. cpVD: circumpapillary vessel density, pfVD: perifoveal vessel density, IN: inferior nasal, NL: nasal lower, NU: nasal upper, SN: superonasal, ST: superotemporal, TU: temporal upper, TL: temporal lower, IT: inferior temporal, SUP: superior, TEM: temporal, INF: inferior, NAS: nasal.

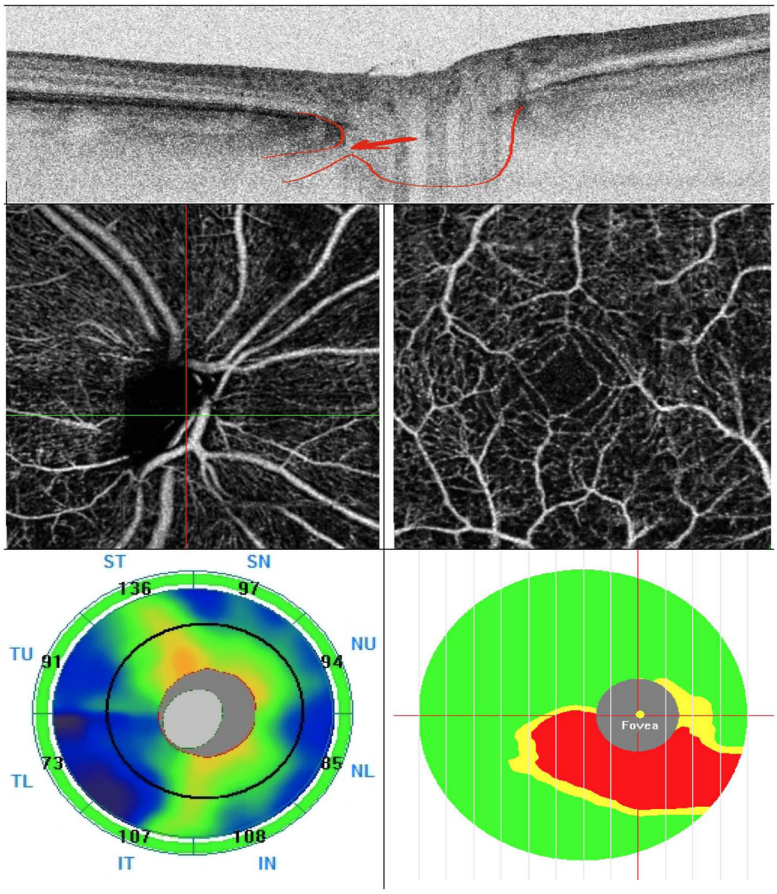

Figure 2.

A representative glaucoma eye with lamina cribrosa defect. Top: Lamina cribrosa defect is seen in horizontal B-scan image of the swept source (SS)-OCT. Middle: Optical coherence tomography angiography (OCT-A) Vessel density map of the peripapillary retinal nerve fiber layer (RNFL) (left) and macular superficial layer (right)) illustrating reduced vessel density. Bottom: optic nerve head thickness map (left) and macular ganglion cell complex (mGCC) thickness map (right). Note that peripapillary RNFL thickness is within normal limit in all sectors but mGCC thickness map shows thickness loss.

Table 1

Demographics and Ocular Characteristics of the Study Population[^]

	Eyes with Focal LC Defect (46 Eyes, 46 Patients)	Eyes without Focal LC Defect (54 Eyes, 54 Patients)	P Value
Age (yrs)	71.45 (67.37, 75.53)	70.82 (67.99, 73.65)	0.794**
Gender (male/female)	16/30	33/21	0.009[ǂ]
Race, n	African American 9 Caucasian 7 White 24 Other 13	African American 10 White 31 Other 13	0.656[ǂ]
Self-reported diabetes, n (%)	6 (13.0)	1 (1.8)	0.029[ǂ]
Self-reported hypertension, n (%)	19 (41.3)	27 (50.0?)	0.384[ǂ]
Spherical Equivalent (D)	−1.13 (−1.73, −0.53)	−0.64 (−1.13, −0.15)	0.204 *
CCT (μm)	533.28 (520.50, 546.06)	534.04 (523.91, 544.18)	0.923[¥]
IOP (mmHg)	14.48 (12.81, 16.16)	14.27 (13.05, 15.51)	0.835[¥]
Axial length (mm)	24.14 (23.64, 24.66)	24.03 (23.68, 24.38)	0.702[¥]
SBP (mmHg)	127.02 (122.03, 132.02)	125.16 (121.04, 129.29)	0.560[¥]
DBP (mmHg)	80.19 (77.04, 83.35)	77.29 (74.62, 79.97)	0.160[¥]
MOPP (mmHg)	54.78 (52.12, 57.46)	52.97 (51.12, 54.82)	0.247[¥]
VF MD (dB)	−5.63 (−7.47, −3.80)	−4.64 (−6.20, −3.08)	0.404 *
VF PSD (dB)	5.68 (4.52, 6.84)	4.79 (3.80, 3.05)	0.242 *
Disc area (mm^2)	2.03 (1.91, 2.15)	2.05 (1.93, 2.18)	0.782[¥]
RNFL thickness (μm)	76.14 (72.45, 79.83)	78.79 (74.65, 82.93)	0.347[¥]

[^]Unless otherwise indicated, continuous variables are shown as mean (95% CI)

LC: lamina cribrosa; D: diopters; CCT: central corneal thickness; IOP: intraocular pressure; SBP: systolic blood pressure; DBP: diastolic blood pressure; MOPP: mean ocular perfusion pressure; VF MD: visual field mean deviation; VF PSD: visual field pattern standard deviation; dB: decibels; RNFL: retinal nerve fiber layer.

*Comparison was performed by using the Mann Whitney test.

ǂComparison was performed by using the chi-square test.

¥Comparison was performed by using independent samples t test.

Table 2

Comparison of Optical Coherence Tomography Angiography Macular Vessel Density and Macular Thickness between the Primary Open-Angle Glaucoma Subjects with and without a Focal Lamina Cribrosa Defect.

	Glaucoma Eyes with Focal LC Defect (46 Eyes, 46 Patients)	Glaucoma Eyes without Focal LC Defect (54 Eyes, 54 Patients)	P Value
wiVD	49.12 (47.93, 50.30)	48.55 (47.45, 49.65)	0.490
pfVD	51.62 (50.40, 52.84)	50.86 (49.73, 51.98)	0.363
Superior hemifield VD	52.08 (50.85, 53.31)	50.92 (49.79, 52.04)	0.173
Inferior hemifield VD	51.15 (49.85, 52.45)	50.78 (49.59, 51.97)	0.682
Temporal sector VD	50.10 (48.86, 51.34)	50.02 (48.87, 51.17)	0.932
Superior sector VD	52.89 (51.57, 54.21)	51.45 (50.23, 52.68)	0.118
Nasal sector VD	52.25 (50.88, 53.63)	50.84 (49.58, 52.11)	0.137
Inferior sector VD	51.21 (49.79, 52.64)	51.09 (49.77, 52.41)	0.900
mGCC (μm)	80.79 (77.40, 84.17)	81.33 (78.23, 84.42)	0.817
Superior Avg (μm)	83.82 (80.16, 87.48)	81.98 (78.64, 85.32)	0.463
Inferior Avg (μm)	77.77 (73.48, 82.05)	80.67 (76.76, 84.59)	0.323
GCC-FLV (%)	7.21 (5.71, 8.71)	4.97 (3.60, 6.35)	
GCC-GLV (%)	16.47 (13.60, 19.35)	14.96 (12.38, 17.59)	0.442

LC: lamina cribrosa; wiVD: whole image vessel density; pfVD: parafoveal vessel density; VD: vessel density; mGCC: macular ganglion cell complex; Avg: average; FLV: focal loss volume; GCC: ganglion cell complex; GLV: global loss volume; Continuous variables are shown as mean (95% CI). The OCT-A parameters between eyes with and without a focal LC defect were compared using independent samples t test.

Table 3

Relationship of Optical Coherence Tomography Angiography Circumpapillary Vessel Density in the Same Peripapillary Sector with LC Defect to the Macular Vessel Density and Thickness.

	IT VD (%) in Glaucoma Eyes with Focal IT LC Defect (39 Eyes, 39 Patients)		ST VD (%) in Glaucoma Eyes with Focal ST LC Defect (17 Eyes, 17 Patients)	
	R^2	P value	R^2	P value
wiVD	0.189	0.005	0.018	0.610
pfVD	0.150	0.015	0.018	0.607
Superior hemifield VD	0.051	0.166	0.014	0.648
Inferior hemifield VD	0.265	0.0008	0.016	0.627
Temporal sector VD	0.164	0.010	0.093	0.231
Superior sector VD	0.044	0.195	0.007	0.746
Nasal sector VD	0.046	0.191	0.0007	0.915
Inferior sector VD	0.293	0.0004	0.006	0.762
mGCC (μm)	0.148	0.017	0.421	0.005
Superior Avg (μm)	0.023	0.363	0.573	0.0004
Inferior Avg (μm)	0.165	0.011	0.066	0.320
GCC-FLV (%)	0.461	<0.0001	0.319	0.018
GCC-GLV (%)	0.406	<0.0001	0.410	0.006

LC: lamina cribrosa; IT: inferotemporal; ST: superotemporal; VD: vessel density; wiVD: whole image vessel density; pfVD: parafoveal vessel density; mGCC: macular ganglion cell complex; Avg: average; FLV: focal loss volume; GCC: ganglion cell complex; GLV: global loss volume.